Microstructures and Wear Resistance of Al-25 wt.%Si Coatings Prepared by High-Efficiency Supersonic Plasma Spraying

Zi-ang Jin[1] · Li-na Zhu[1,4] · Hai-dou Wang[1,2] · Ming Liu[2] · Jia-jie Kang[1,4] · Guo-zheng Ma[2] · Shu-ying Chen[3]

Abstract Hypereutectic Al-Si alloy is an ideal surface strengthening material for aluminum alloy cylinder body. However, the coarse eutectic silicon phase and primary silicon particles in Al-Si alloys prepared by traditional methods lead to poor mechanical properties of the alloys, and the high cost of preparation limits the practical application of hypereutectic Al-Si alloys. In this study, Al-25 wt.%Si coatings were prepared on substrate 7075 by high-efficiency supersonic plasma spraying (HESP). The micromorphology, Vickers hardness, bonding strength and wear resistance of the coatings were measured and characterized by experiments. The results show that the Al-25 wt.%Si coatings prepared by HESP have a denser structure, and the primary silicon phase in the coatings is refined. The hardness of the coatings is 235 $HV_{0.1}$, and the bonding strength between the coatings and the substrate is 44.1 MPa. The wear rate of the coatings is reduced by 20 times compared with that of the substrate, and the wear mechanism is mainly adhesion wear and oxidation wear.

✉ Li-na Zhu
zhulina@cugb.edu.cn

Hai-dou Wang
wanghaidou@aliyun.com

1 School of Engineering and Technology, China University of Geosciences (Beijing), Beijing 100083, China

2 National Key Lab for Remanufacturing, Army Academy of Armored Forces, Beijing 100072, China

3 National Key Laboratory of Human Factors Engineering, China Astronaut Research and Training Center, Beijing 100094, China

4 Zhengzhou Institute, China University of Geosciences (Beijing), Zhengzhou 451283, China

Introduction

Nowadays, with the development of automobiles, the use of aluminum engine is more and more widespread. The aluminum engine is to prepare a wear-resistant coating on the surface of aluminum alloy cylinder body to enhance its wear resistance. Hypereutectic Al-Si alloys have the advantages of lightweight, high stiffness, excellent wear resistance and low thermal expansion coefficient (Ref 1-3). It is an ideal surface strengthening material for aluminum alloy cylinder body. Hypereutectic Al-Si alloy generally refers to Al-Si alloys with silicon content greater than 13%. Related studies have shown that (Ref 4-7), silicon content has a significant effect on wear behavior of Al-Si alloys. With the increase in silicon content to eutectic compound, wear resistance is improved. At the same time, the shape, size and distribution of eutectic silicon phase and primary silicon also affect the properties of hypereutectic Al-Si alloys. At present, casting and spraying deposition are the main methods to prepare Al-Si alloys (Ref 8-10). However, due to the relatively low solidification rate during the casting process, hypereutectic Al-Si alloys prepared by the conventional casting method result in the formation of a needlelike eutectic silicon phase and rectangular-shaped coarse primary silicon, which seriously deteriorates the mechanical properties of alloys and hinders their practical application. Spraying deposition technology is usually used to prepare hypereutectic Al-Si alloys by rapid cooling and solidification (Ref 11, 12). It can improve the microstructure of Al-Si alloys and refine the eutectic silicon phase and primary silicon. However, the preparation conditions are

severe, and some complicated technique and expensive equipment must be used, which limits its actuality application (Ref 13, 14).

Compared with the traditional method of preparing high Al-Si alloy, other researchers use thermal spraying technology to prepare a layer of high Al-Si coatings on the surface of aluminum alloy, the surface hardness and wear resistance of the aluminum alloy can be improved, and its application in automobile engine can reduce the cost and improve the efficiency. Yi et al. (Ref 15) studied on the Al-12 wt.%Si coatings were fabricated using cold spray technique and the results showed that the hardness of the coatings was $120HV_{0.1}$. XIE et al. (Ref 16) studied on the Al-13 wt.%Si coatings were fabricated using droplet spraying process and the results showed that the hardness of the coatings was $170HV_{0.1}$. Laha et al. (Ref 17) studied on the Al-23 wt.%Si coatings were fabricated using high-velocity oxy-fuel spray technology and the results showed that the hardness of the coatings was $193HV_{0.1}$ and the porosity of the coatings was 3.2%.

As an important technology in surface engineering and remanufacturing engineering, the HESP adopts the single anode structure of Laval nozzle profile, and plasma jet is formed by arc ionization of inert gas (argon) between the anode and cathode. As the length of nozzle channel is compressed and the mechanical compression of the initial arc is enhanced, the anode spots are forced to move forward and elongate the arc (the arc voltage can reach 200-400 V). The thermal efficiency of the spraying gun is improved. The spraying temperature is as high as 10,000 C, and the flying speed of particles is as high as 400-600 m/s. The spray nozzle adopts an inner powder feeding structure, and the spray material is sent to the plasma jet for heating and acceleration. When the molten particles collide with the substrate, they are cooled and solidified rapidly to form a coating. The inert gas (argon) is used in spraying gas, which can reduce particle oxidation and form fewer defects and high-quality coatings. Compared with the traditional thermal spraying technology, HESP technology can obtain high-quality Al-Si coatings. Thus, HESP technology has broad prospects in practical production and application.

In this study, Al-25 wt.%Si coatings were prepared by HESP technology. The microstructure, mechanical properties and wear properties of the coatings were studied experimentally.

Experimental Materials and Method

Preparation of Coatings

The spraying raw material was Al-25 wt.%Si powders (silicon content is 25 wt.%) produced by Changsha Tianjiu Metal Material Co., Ltd., China, using gas atomization, and the powder morphology is shown in Fig. 1. The substrate is 7075 with a size of 50 mm × 10 mm × 3 mm, and the main composition of substrate 7075 is shown in Table 1. Before the experiment, the Al-25 wt.%Si powders were dried for 3 h at 100 °C in the dry box, and the substrate 7075 was cleaned ultrasonically for 30 min in a bath of acetone to remove oil stain. Then, the surface of the substrate was grit blasted to $R_a \approx 6$ μm by a manual blasting machine, using 500-μm angular alumina grits, to increase the bonding strength between coatings and the substrate. Finally, the Al-25 wt.%Si coatings were fabricated using HESP developed by National Key Laboratory for Remanufacturing, China. The spraying method is to stop spraying after one spraying, then cool the substrate to room temperature with cooling gas, then spray for the second time and then cycle in turn until the coating thickness is 0.4 mm to finish spraying. The internal structure of the HESP gun is shown in Fig. 2, and the process parameters of grit blasting and spraying are given in Table 2.

Characterization of Coatings

The surface morphology, cross section morphologies and composition of the coatings were analyzed by Nova NanoSEM50-type environmental scanning electron microscope (SEM, FEI, America) equipped with energy-dispersive spectroscopy (EDS, OXFORD, England). The phase identification of the samples was conducted by x-ray diffraction (XRD, Bruker, Germany) device with Cu Kα radiation. The tube voltage and current were 40 kV and 150 mA, respectively. The scanning speed and range were 3°/min and 20° ∼ 90°, respectively. Talos-F200X field emission transmission electron microscope (TEM, FEI, Talos-F200X, America) was used for the coating's crystal structure and high-resolution image.

The porosity of Al-25 wt.%Si coatings was measured by grayscale method. The pore size inside the coatings was expressed by their area distribution on the two-dimensional plane. The main steps were as follows: acquisition of 1000 × magnification SEM images of 10 coatings section, input ImageJ2x software, transformation images, processing images and recording porosity.

The microhardness of coatings was measured using a microhardness tester (MICROMET-6030, Buehler, America) with load 100 gf and hold time 15 s. The bonding strength of the coatings was tested according to ASTMC-633-01 standard. The coatings sample was bonded with the stretching fixture (35CrMo steel) by using E-7 glue (E-7, Shanghai Huayi, China). After E-7 solidification, it was measured on MTS809 universal tensile testing machine. The cross-head speed of the equipment was 1 mm/min. The bonding strength of each coating is the average of

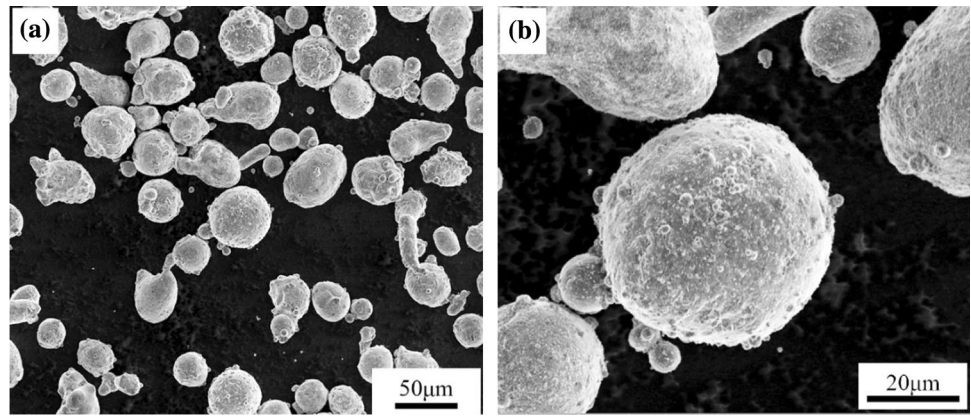**Fig. 1** Micromorphology of the Al-25 wt.%Si powders: (a) low magnification and (b) high magnification

Table 1 Chemical composition of substrate 7075 (mass fraction, %)

Element	Mg	Zn	Cu	Cr	Fe	Mn	Si	Ti	Al
Wt.%	2.1-2.9	5.1-6.1	1.2-2.0	0.18-0.28	≤ 0.5	≤ 0.3	≤ 0.4	≤ 0.2	Balance

Fig. 2 Internal structure of the HESP gun
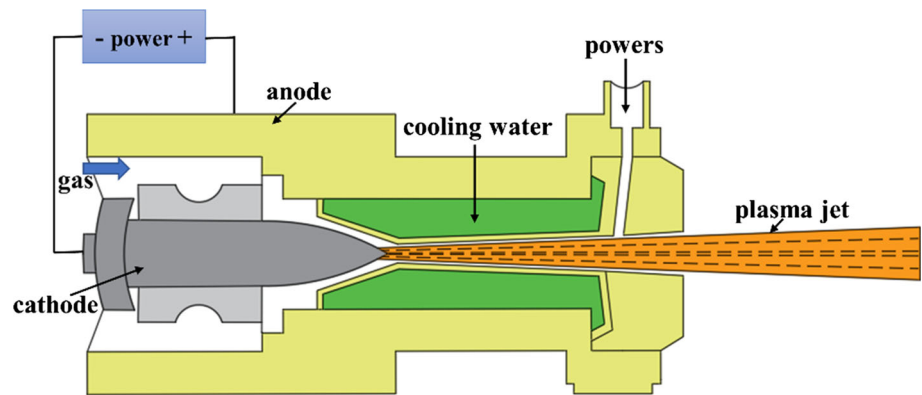
Table 2 Spraying and grit-blasting parameters

Process	Parameters	Values
Grit blasting	Air pressure, MPa	0.7
	Blasting distance, mm	300
	Blasting angle, °	90
	Voltage, V	135
HESP	Current, A	350
	Spraying distance, mm	100
	Cooling of substrate	Air blow
	Gas flow rate, L/min	Ar(120), H$_2$(13)
	Coating thickness, mm	0.40

three experimental measurements. Tensile test specimen (diameter is 25.4 mm) is shown in Fig. 3.

Friction and Wear Test

The wear resistance tests were carried out on a UMT-3 multi-functional friction and wear tester (CETR, America), as shown in Fig. 4. The samples of the coatings are 10 × 10 × 3 mm. The diameter of the GCr15 ball was 4 mm, and its Rockwell hardness was 61 HRC. In order to ensure the consistence of the experimental conditions, the samples were grinded with SiC sandpaper from #400 to #1000 before the experiment, until the surface roughness (R_a) of the sample was less than 0.8 μm and then polished. The experimental parameters were: load 2 N; frequency 2 Hz; test time 20 min; amplitude 4 mm. The morphologies and section profiles of the worn surfaces were characterized by means of SEM and LEXT (Olympus OLS4000, Japan) 3D laser measuring microscope.
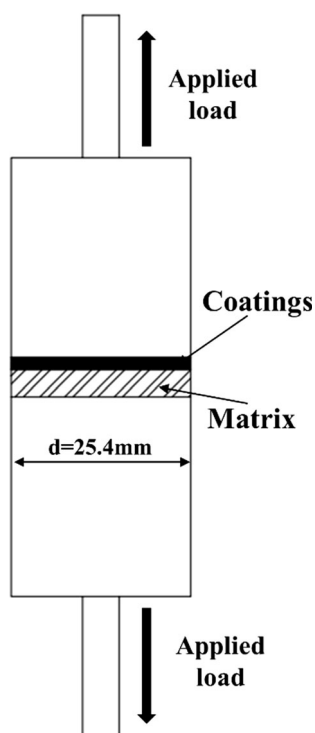
Fig. 3 Tensile test specimen for measuring bond strength of spray coatings
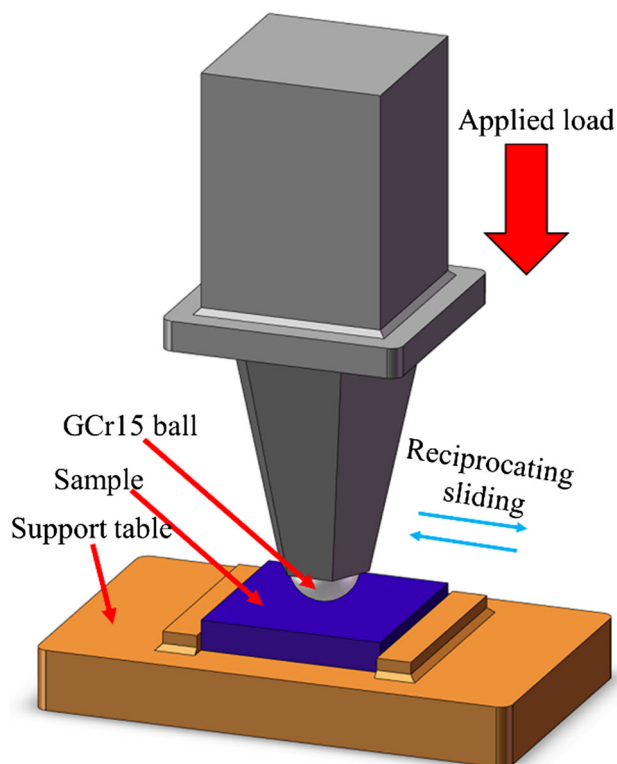

Fig. 4 Schematic diagram of the friction pair for linear reciprocating sliding contact

Results and Discussion

Surface and Cross-Sectional Morphology

The typical surface topography of the Al-25 wt.%Si coatings is shown in Fig. 5(a). The particles melt well, spread evenly, and the coating surface is denser with a few pores. The cross-sectional morphology of Al-25 wt.%Si coatings is shown in Fig. 5(b). The coatings have compact structure, and there are no large pores and impurities, only a small number of micropores, and no cracks at the interface between the coatings and the substrate, which is a typical mechanical bonding mode (Ref [18]). The measured porosity of the coatings is 2.02%. This is attributed to HESP spraying technology, which has high flame temperature, good melting state and high-flying speed of particles. When molten or semi-molten particles reach the substrate, they have high kinetic energy and thermal enthalpy, and strong impact force, making them fully flattened and evenly spread.

The TEM image of Al-25 wt.%Si coatings is shown in Fig. 6(a). Some spherical and bulk particles appear in the coatings. The EDS scanning of the coatings (in Fig. 6b) indicates that only Al and Si elements were found in the coatings, and the distribution of both elements was very uniform. Moreover, the EDS analysis of these spherical and bulk particles shows that the silicon content is very high, so we can judge that these spherical and bulk particles are primary silicon phase. SAED patterns (in Fig. 6a) insinuate the presence of aluminum and silicon in Al-25 wt.%Si coatings. The less intense, but well-defined ring pattern indicates the presence of ultrafine crystalline structure. The average grain size was estimated from the x-ray diffraction spectra using Scherer's formula and the size range of primary silicon phase in Al-25 wt.%Si coatings was 50-120 nm. Compared with the coarse bulk or rod-shaped primary silicon with the size range of 40-200 μm of high Al-Si alloys prepared by conventional casting method, the size range of block primary silicon phase of high Al-Si alloys prepared by spraying deposition technology is 10-30 μm (Ref [1], [19]), indicating that the primary silicon phase of Al-25 wt.%Si coatings prepared by HESP is refined. This is attributed to the fact that the spraying heating temperature of HESP ranges from 5000 to 11,000 °C. When Al-25 wt.%Si powders are heated at high temperature and flying at high speed, they impact on the substrate and are cooled by cooling gas in a very short time (10^6-10^8 K/s) (Ref [17]) and then rapidly solidify to form coatings. Under this extremely hot and cold spraying condition, the growth of primary silicon phase is limited. However, there is no eutectic silicon phase in the Al-

Fig. 5 Microstructure and morphology of Al-25 wt.%Si coatings: (a) surface morphology and (b) cross-sectional morphology
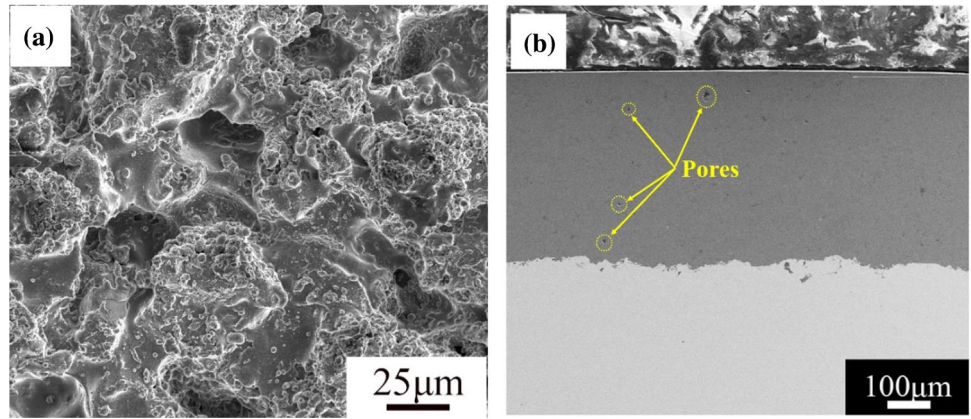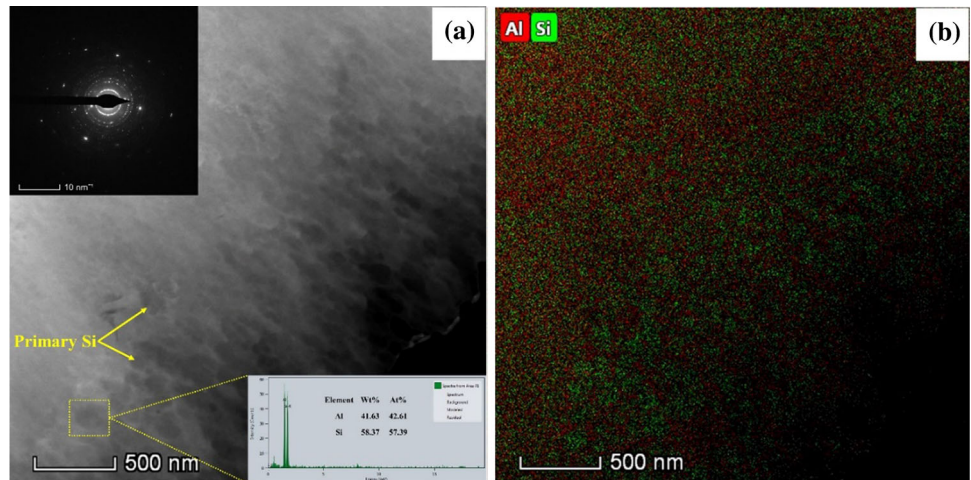

Fig. 6 TEM morphology and EDS of Al-25 wt.%Si coatings: (a) TEM morphology and (b) EDS surface scanning

25 wt.%Si coatings. This is because the cooling time of droplets is too short to form eutectic silicon phase.

XRD Analysis

The XRD patterns of Al-25 wt.%Si powders and Al-25 wt.%Si coatings are shown in Fig. 7. It can be seen from the patterns that the phases of the powders and coatings are identical, all of which are aluminum, silicon and $Al_{3.21}Si_{0.47}$.

Mechanical Property

Five points were selected to measure the hardness of coatings and substrates. The microhardness values of Al-25 wt.%Si coatings and substrate 7075 are shown in Table 3. The average microhardness of coatings is 235 $HV_{0.1}$, which is 2.2 times higher than that of substrate 107.4 $HV_{0.1}$. This is because the presence of nanosized grains in the Al-25 wt.%Si coatings will result in higher mechanical strength of coatings. These nanosized primary silicon phase can act as potential barrier for dislocation
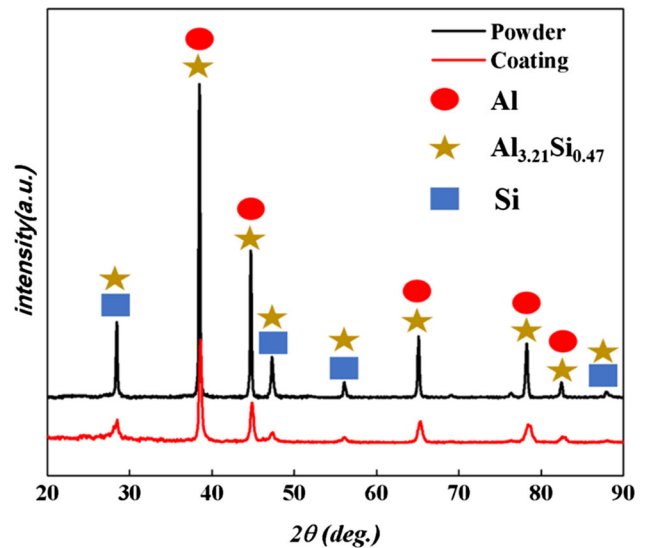

Fig. 7 XRD patterns of Al-25 wt% Si powders and coatings

movement and thus can improve the mechanical strength and hardness of the Al-25 wt.%Si coatings, which can improve the wear resistance of the coating (Ref 20, 21).

Table 3 Vickers hardness of Al-25 wt.%Si coatings and substrate 7075

	1	2	3	4	5	Average value
Coatings ($HV_{0.1}$)	234.3	236.8	231.9	236.8	235.2	235.0
Substrate ($HV_{0.1}$)	103.2	108.4	107.9	107.9	109.5	107.4

Fig. 8 Tensile fracture morphology of Al-25 wt% Si coatings samples

Table 4 Bonding strength between Al-25 wt.%Si coatings and substrate 7075

	1	2	3	Average value
Bonding strength, MPa	45.2	43.6	43.5	44.1

Fig. 9 Friction coefficient with time for Al-25 wt.%Si coatings and substrate 7075

Through tensile test, all three samples were disconnected at the interface between coatings and substrate (in Fig. 8). The bonding strength between coatings and substrate is shown in Table 4. The three bonding strength values between coatings and substrate are 45.2 MPa, 43.6 MPa and 43.5 MPa, and the average value is 44.1 MPa, which is higher than the 30 MPa bonding strength between the Al-Si coatings and aluminum alloy substrate prepared by traditional thermal spraying technology (high-velocity oxy-fuel spray technology and common plasma spraying technology, etc.) (Ref 22). Porosity, oxide and impurities in the coatings have a great influence on the bonding strength of the coatings (Ref 23). As Al-25 wt.%Si coatings prepared by HESP is uniform and compact, the bonding strength between coatings and substrate is better.
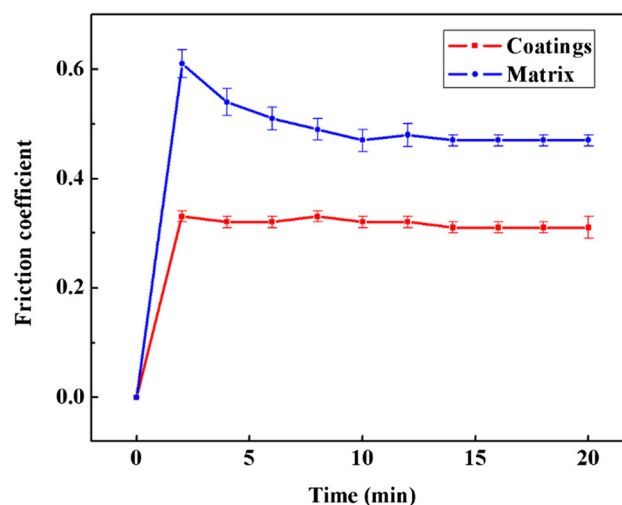
Friction and Wear Properties

Friction Coefficient

The friction coefficient curves of Al-25 wt.%Si coatings and substrate 7075 are shown in Fig. 9. Three friction tests were carried out on each specimen, and the average values of friction coefficients were obtained, and the trend of friction coefficients was the same. The friction coefficient of the substrate increases sharply at the initial stage of friction and tends to be stable gradually. The reason for this trend is that in the initial stage of friction, the friction coefficient rises sharply because the wear surface is rough

and the contact between GCr15 ball and substrate 7075 surface is not uniform. With the development of friction, the contact between GCR15 ball and substrate 7075 surface becomes tight and the friction coefficient tends to be stable. The friction coefficient of Al-25 wt.%Si coatings is generally stable and is significantly lower than that of substrate 7075. This indicates that the Al-25 wt.%Si coatings have a good anti-friction performance compared with substrate 7075.

Wear Rate

Figure 10 shows the three-dimensional morphologies of wear surfaces of Al-25 wt.%Si coatings and substrate 7075. The width and depth of wear tracks of Al-25 wt.%Si coatings and substrate 7075 are shown in Table 5. The wear rate K (mm^3/N m) is calculated by the following formula, and the result is shown in Fig. 9:
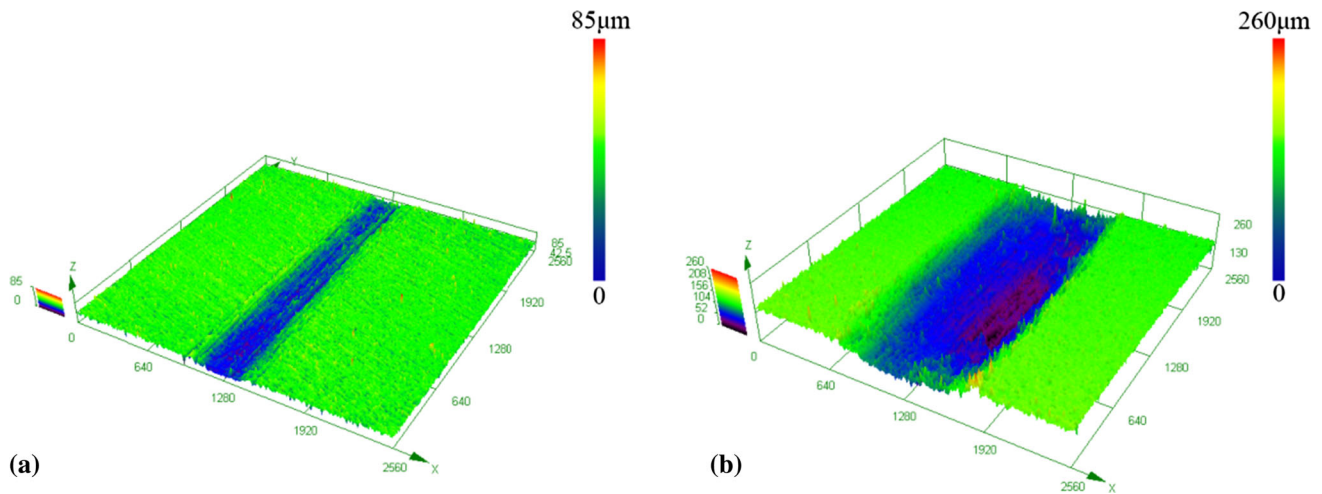
$$K = \frac{S \cdot l}{L \cdot F}$$

Fig. 10 3D morphologies of wear track: (a) Al-25 wt%Si coatings and (b) substrate 7075

Table 5 Width and depth of wear track

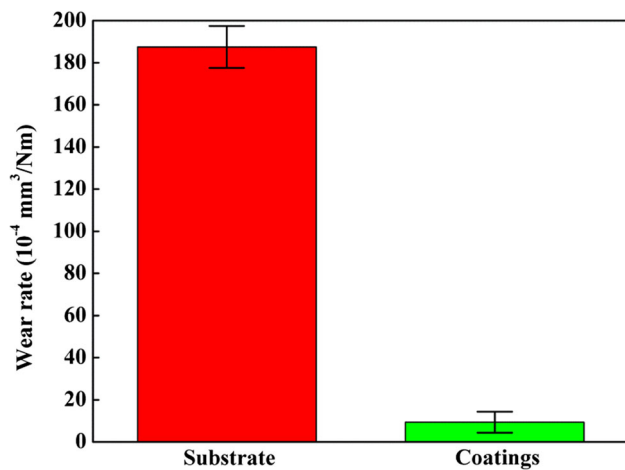|	Width, μm	Depth, μm
Coatings	453.5	16.5
Substrate	1207.1	108.8

Fig. 11 Wear rate of Al-25 wt.%Si coatings and substrate 7075

where S is the area of cross section in mm^2, l is the length of wear track in mm, L is the total sliding distance in m and F is the applied load in N.

It can be seen from Table 5 that the width and depth of the wear track of Al-25 wt.%Si coatings are 453.5 μm and 16.5 μm, respectively, and those of substrate 7075 are 1207.1 μm and 108.8 μm. It can be seen from Fig. 11 that the wear rate of substrate 7075 is 187.5 × 10^{-4} mm^3/N m, which is 20 times higher than that of Al-25 wt.%Si coatings of 9.37 × 10^{-4} mm^3/N m. This is because the
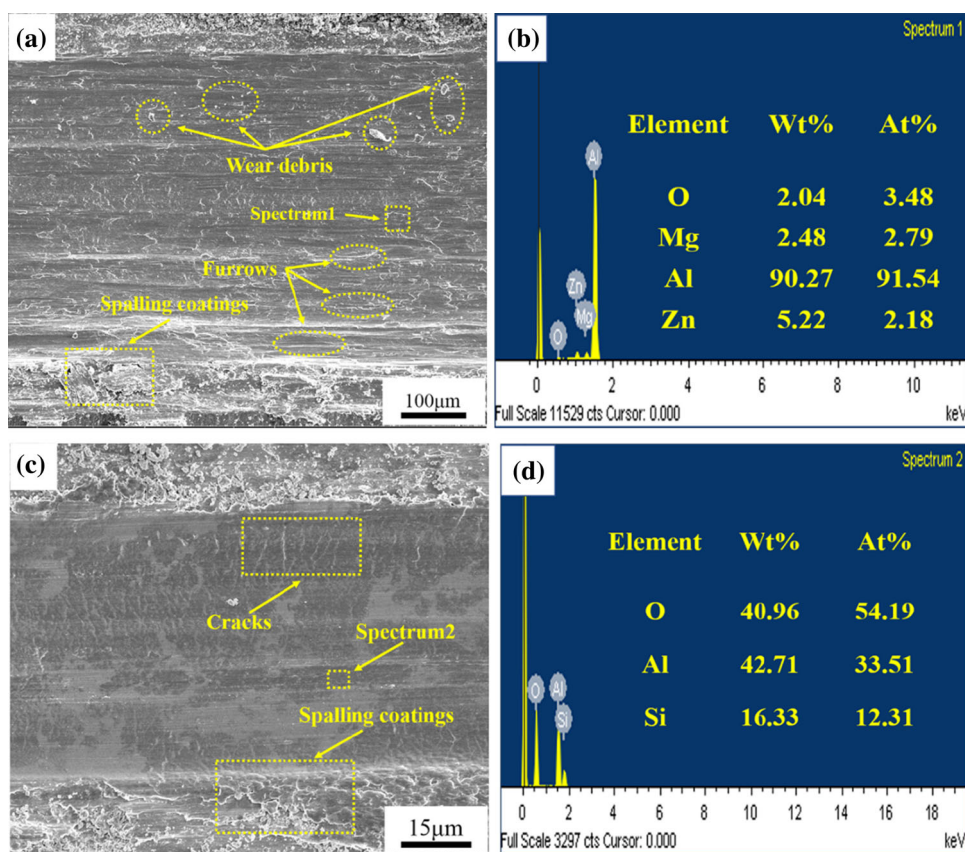
hardness of substrate 7075 is lower than that of Al-25 wt.%Si coatings and is softer than that of coatings. For the softer metals, the wear rate is greatly affected by the wear contact area (Ref 24). As can be seen from Fig. 10 and Table 4, the width and depth of the wear track of the substrate are larger, indicating that the wear contact area is larger and the wear is serious. The hardness of Al-25 wt.%Si coatings is higher than that of substrate 7075. In Al-25 wt.%Si coatings, aluminum-rich phase is a soft substrate, which plays the role of fixing primary silicon phase. In the process of wear, primary silicon phase as hard phase bears load pressure, and reduces grinding depth and friction contact area, which results in lower wear rate.

Wear Mechanism

The SEM diagrams of the wear surfaces of substrate 7075 and Al-25 wt.%Si coatings are shown in Fig. 12(a) and (c). It can be seen from Fig. 12(a) that the wear surface of substrate 7075 is very rough, and there are a lot of furrows, debris and delamination along the direction of the wear track, which indicates that serious abrasive wear and adhesion wear have occurred. This is due to the low hardness and rough surface of substrate 7075. Adhesive wear occurs at the beginning of wear, and shear failure mainly occurs on the surface layer of the soft substrate. As wear progresses, the area of adhesive points between GCr15 ball and substrate surface increases, and many abrasive debris attach to the wear track surface. Serious plastic deformation occurs on the contact wear zone. At the same time, serious abrasive wear occurs and serious scratches occur on the wear surface.

It can be seen from Fig. 12(c) that the wear surface of the Al-25 wt.%Si coatings is smooth. There are obvious cracks in the vertical direction of the wear track, and

Fig. 12 SEM diagrams of the worn surfaces and EDS spectrums: (a) the worn surfaces of substrate 7075; (b) the EDS spectrum of substrate 7075; (c) the worn surfaces of Al-25 wt.%Si coatings; (d) the EDS spectrum of Al-25 wt.%Si coatings

spalling coatings on both sides of the wear track, indicating that adhesive wear has taken place. Because the hardness of Al-25 wt.%Si coatings is higher than that of substrate 7075, the separation force is produced in the direction of the wear track, and cracks are produced along the vertical direction of the wear track. Previous studies have shown that the morphology and size of eutectic silicon phase play an important role in the wear resistance of Al-Si alloys (Ref 25). The primary silicon phase in Al-25 wt.%Si coatings is bulky (Fig. 12c), showing some spheroidizing effects. This effect can effectively reduce the localized stress concentration at the interface of spheroidized silicon/alpha aluminum, making the surface primary silicon and alpha aluminum combine perfectly, and effectively inhibit the crack propagation at the interface of spheroidized silicon/alpha aluminum. At the same time, the spheroidizing effects of primary silicon phase can increase the fracture toughness of the coatings, making the spheroidized silicon/alpha aluminum interface more difficult to fracture. This can effectively reduce the formation of crack nucleation sites and improve the wear resistance of Al-25 wt.%Si coatings.

Through EDS analysis of the wear surface, it can be seen from Fig. 12(b) and (d) that the oxygen element appears on the worn surface of Al-25 wt.%Si coatings and substrate 7075, and the oxygen content on the worn surface

of Al-25 wt.%Si coatings is much higher than that of substrate 7075. The reason is that the temperature at sliding surface interface gradually increases with the sliding continues. Relevant work indicated that the increase in temperature within the limit range can increase the ability of soft aluminum substrate to accommodate hard and brittle polyhedral shaped primary silicon crystals (Ref 26, 27), resulting in a higher hardness of the Al-25%Si coating. Moreover, the formed oxide film reduces the direct contact between GCr15 ball and Al-25 wt.%Si coatings, thus reducing the interaction and enhancing the wear resistance of the coatings. Therefore, oxidation wear also occurs in the Al-25 wt.%Si coatings.

Conclusion

The following main conclusions can be drawn:

(1) High-efficiency supersonic plasma spraying technology has the characteristics of inert heat source, high temperature, high speed and short spraying distance. The Al-25 wt.%Si coatings prepared by this technology is uniform and compact and the coatings mechanically bonded with the substrate. The porosity of Al-25 wt.%Si coatings is 2.02%, the hardness

of Al-25 wt.%Si coatings is 235 $HV_{0.1}$, and the bonding strength between coatings and substrate is 44.1 MPa.

(2) The heat source temperature range of high-efficiency supersonic plasma spraying technology is 5000-11,000 °C, and the substrate temperature is usually controlled at room temperature by cooling gas. Al-25 wt.%Si powders can undergo extremely hot and cold spraying conditions in a very short time (10^6-10^8 K/s), so that the primary silicon phase in Al-25 wt.%Si coatings can be refined, and the size range is 50-120 nm.

(3) Al-25 wt.%Si coatings prepared by high-efficiency supersonic plasma spraying technology have stable and lower friction coefficient, and it has a good anti-friction performance compared with substrate 7075. At the same time, the wear rate of Al-25 wt.%Si coatings is 20 times lower than that of the substrate, indicating it also has a good wear resistance. The main wear mechanisms of the coatings are adhesion wear and oxidation wear.

References

1. F. Huang, L. Hua, X.P. Qin, Z.L. Hu, Z. Wang, Y.L. Song, and Y.X. Liu, Microstructures and Thermal Stabilities of High Silicon Aluminum Alloys Prepared by Spray Deposition, *Appl. Mech. Mater.*, 2014, **711**, p 206-209

2. K. Nakashima, K. Funa, D. Kurokawa, Y. Nakano, Y. Murakami, and M. Yamamoto, Piston Ring Projection and Catching in Cylinder Ports of Two-Stroke Cycle Engine, *J. Adv. Mech. Des. Syst. Manuf.*, 2012, **6**(1), p 23-32

3. L.G. Hou, H. Cui, Y.H. Cai, and J.S. Zhang, Effect of (Mn plus Cr) Addition on the Microstructure and Thermal Stability of Spray-Formed Hypereutectic Al-Si Alloys, *Mater. Sci. Eng. A*, 2009, **527**(1), p 85-92

4. F. Alshmri and H.V. Atkinson, Hardness of Rapidly Solidified Al-High Si Alloys, *Adv. Mater. Res.*, 2012, **476–478**, p 2476-2480

5. Y.X. Li, J.Y. Liu, W.S. Wang, and G.Q. Liu, Microstructures and Properties of Al-45%Si Alloy Prepared by Liquid-Solid Separation Process and Spray Deposition, *Trans. Nonferrous Met. Soc. China*, 2013, **23**(4), p 970-976

6. M. Elmadagli, T. Perry, and A.T. Alpas, A Parametric Study of the Relationship Between Microstructure and Wear Resistance of Al-Si Alloys, *Wear*, 2007, **262**(1–2), p 79-92

7. M. Chen, X. Meng-Burany, T.A. Perry, and A.T. Alpas, Micromechanisms and Mechanics of Ultra-mild Wear in Al-Si Alloys, *Acta Mater.*, 2008, **56**(19), p 5605-5616

8. Y. Liu, J. Yin, and Y. Zhong, Microstructure and Wear Properties of Al-20Si Alloy Prepared by Spray Deposition with Following Continuous Extrusion Forming Technique, *Mater. Res. Express*, 2016, **3**(10), p 106502. https://doi.org/10.1088/2053-1591/3/10/106502

9. K.N. Prabhu and B.N. Ravishankar, Effect of Modification Melt Treatment on Casting/Chill Interfacial Heat Transfer and Electrical Conductivity of Al-13% Si Alloy, *Mater. Sci. Eng. A*, 2003, **360**(1–2), p 293-298

10. W.X. Shi, B. Gao, G.F. Tu, and S.W. Li, Effect of Nd on Microstructure and Wear Resistance of Hypereutectic Al-20%Si Alloy, *J. Alloys Compd.*, 2010, **508**(2), p 480-485

11. C. Cui, A. Schulz, K. Schimanski, and H.W. Zoch, Spray Forming of Hypereutectic Al-Si Alloys, *J. Mater. Process. Technol.*, 2009, **209**(11), p 5220-5228

12. F. Wang, Y.J. Ma, Z.Y. Zhang, X.H. Cui, and Y.S. Jin, A Comparison of the Sliding Wear Behavior of a Hypereutectic Al-Si Alloy Prepared by Spray-Deposition and Conventional Casting Methods, *Wear*, 2004, **256**(3–4), p 342-345

13. L.D. Wang, D.Y. Zhu, Z.L. Wei, Y.L. Chen, L.G. Huang, Q.J. Li, and Y.S. Wang, Effect of the Mixing-Melt and Superheating on the Primary Si Phase of Hypereutectic Al-20%Si Alloy, *Adv. Mater. Res.*, 2011, **146–147**, p 79-88

14. Q.L. Li, T.D. Xia, Y.F. Lan, and P.F. Li, Effects of Melt Superheat Treatment on Microstructure and Wear Behaviours of Hypereutectic Al-20%Si Alloy, *Mater. Sci. Technol.*, 2014, **30**(7), p 835-841

15. H.Y.J.Q. Wang, X.Y. Cui, J. Wu, T.F. Li, and T.Y. Xiong, Microstructure Characteristics and Mechanical Properties of Al-12Si Coatings on AZ31 Magnesium Alloy Produced by Cold Spray Technique, *J. Therm. Spray Technol.*, 2016, **25**(5), p 1020-1028

16. K. Xie, M.Q. Cao, P.C. Xia, and L.J. Yue, Improving Wear Resistance of Magnesium by Droplet Spraying of Al-Si Alloy, *J. Cent. South Univ. Technol.*, 2013, **20**(7), p 1781-1785

17. T. Laha, Y. Liu, and A. Agarwal, Carbon Nanotube Reinforced Aluminum Nanocomposite via Plasma and High Velocity Oxy-Fuel Spray Forming, *J. Nanosci. Nanotechnol.*, 2007, **7**(2), p 515-525

18. S.J. Kim and Y.B. Woo, Coating Layer and Corrosion Protection Characteristics in Sea Water with Various Thermal Spray Coating Materials for STS304, *Surf. Rev. Lett.*, 2010, **17**(3), p 299-305

19. S.C. Hogg, A. Lambourne, A. Ogilvy, and P.S. Grant, Microstructural Characterisation of Spray Formed Si-30Al for Thermal Management Applications, *Scr. Mater.*, 2006, **55**(1), p 111-114

20. H.V. Atkinson, F.D. Alshmri, S.V. Hainsworth, and S.D.A. Lawes, Microstructural Characterization of Rapidly Solidified Al-High Si Alloys, *Adv. Mater. Res.*, 2011, **328–330**, p 1545-1551

21. C.L. Xu, Y.F. Yang, H.Y. Wang, and Q.C. Jiang, Effects of Modification and Heat-Treatment on the Abrasive Wear Behavior of Hypereutectic Al-Si Alloys, *J. Mater. Sci.*, 2007, **42**(15), p 6331-6338

22. K. Nakata and M. Ushio, Wear Resistance of Plasma Sprayed Al-Si Binary Alloy Coatings on A6063 Al Alloy Substrate, *Surf. Coat. Technol.*, 2001, **142–144**, p 277-282

23. Z. Glogovic, Z. Kozuh, and S. Kralj, A Mathematical Model for the Calculation of the Adhesion of a Flame Sprayed Coating of Aluminum on S 235 JR Steel, *J. Therm. Spray Technol.*, 2012, **21**(1), p 63-76

24. J.H. Jang, B.D. Joo, J.H. Lee, and Y.H. Moon, Effect of Hardness of the Piston Ring Coating on the Wear Characteristics of Rubbing Surfaces, *Met. Mater. Int.*, 2009, **15**(6), p 903-908

25. Y.D. Li, M.T. He, S.H. Hu, J.L. Suo, and Y. Ma, Effects of Mixing Melt Treatment and Heat-Treatment on the Microstructure and Wear Resistance of Al-22%Si Alloys, *Adv. Mater. Res.*, 2013, **815**, p 195-200

26. D.K. Dwivedi, Wear Behaviour of Cast Hypereutectic Aluminium Silicon Alloys, *Mater. Des.*, 2006, **27**(7), p 610-616
27. M.M. Haque, N.I. Syahriah, and A.F. Ismail, Effect of Silicon on Strength and Fracture Surfaces of Aluminium-Silicon Casting and Heat Treated Alloys, *Key Eng. Mater.*, 2006, **306–308**, p 893-898